

Detailed Investigation of the OH Radical Quenching by Natural Antioxidant Caffeic Acid Studied by Quantum Mechanical Models

Monica Leopoldini, Sandro G. Chiodo, Nino Russo,* and Marirosa Toscano

Dipartimento di Chimica and Centro di Calcolo ad Alte Prestazioni per Elaborazioni Parallele e Distribuite-Centro d'Eccellenza MIUR, Università della Calabria, I-87030 Arcavacata di Rende (CS), Italy

 Supporting Information

ABSTRACT: The effectiveness of naturally occurring antioxidant caffeic acid in the inactivation of the very damaging hydroxyl radical has been theoretically investigated by means of hybrid density functional theory. Three possible pathways by which caffeic acid may inactivate free radicals were analyzed: hydrogen abstraction from all available hydrogen atoms, hydroxyl radical addition to all carbon atoms in the molecule, and single electron transfer. The reaction paths were traced independently, and the respective thermal rate constants were calculated using variational transition-state theory including the contribution of tunneling. The more reactive sites in caffeic acid are the C₄OH phenolic group and the C₄ carbon atom, for the hydrogen abstraction and radical addition, respectively. The single electron transfer process seems to be thermodynamically unfavored, in both polar and nonpolar media. Both hydrogen abstraction and radical addition are very feasible, with a slight preference for the latter, with a rate constant of $7.29 \times 10^{10} \text{ M}^{-1} \text{ s}^{-1}$ at 300 K. Tunnel effects are found to be quite unimportant in both cases. Results indicate caffeic acid as a potent natural antioxidant in trapping and scavenging hydroxyl radicals.

1. INTRODUCTION

Phenolic compounds are plant secondary metabolites, and they are commonly found in herbs and fruits such as berries, apples, citrus fruit, cocoa, and grapes; vegetables like onions, olives, tomatoes, broccoli, lettuce, and soybeans; grains and cereals; green and black teas; coffee beans; propolis; and red and white wines.^{1–8}

Phenolic compounds are synthesized in the secondary metabolism of plants from two major synthetic pathways: the shikimate and the acetate pathway.⁹

Plants have evolved to produce phenolic compounds compounds to protect against fungal parasites,¹⁰ herbivores, pathogens, and oxidative cell injury.¹¹ Furthermore, they produce stimuli to assist in pollination¹² and guide insects to their food source.¹⁰

In recent decades, phenolic compounds have attracted growing global interest upon the discovery of the so-called “French Paradox”, i.e., the observation that although the French have a tendency to smoke and a diet rich in fats, they show much reduced rates of coronary heart diseases when compared with other northern European nations.¹³ The most popular explanation has been recognized in the relatively high daily consumption of red wines rich in phenolic compounds by the French, which in some way protects them from heart disease.^{1,14}

The term phenolics encompasses approximately 8000 naturally occurring compounds, all having a phenol ring. A further classification divides them in polyphenols and simple phenols, depending on the number of phenol subunits. Simple phenols include phenolic acids.¹⁵ Polyphenols possessing at least two phenol subunits include the flavonoids and the stilbenes. Those compounds with three or more phenol subunits are referred to as the tannins.¹⁶

The pharmacological, medicinal, and biochemical properties of phenolics have been extensively reviewed.^{17–19} They have

been reported to have antioxidant,²⁰ vasodilatory, anticarcinogenic, antinflammatory, immune-stimulating, antiallergic, and antiviral and estrogenic effects.^{21,22} In addition, inhibition activities against several enzymes like phospholipase A₂, cyclooxygenase, lipoxygenase,^{23–30} glutathione reductase,³¹ and xanthine oxidase enzymes³² were proven.

A diet rich in fruits and vegetables that contain these compounds reduces the risk of cardiovascular and some other diseases, and most countries have developed recommendations for an increased intake of fruit and vegetables.³³

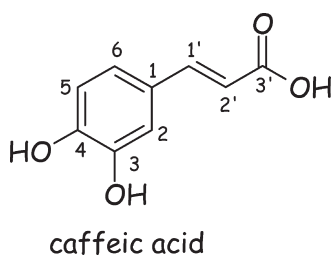
The best described property of phenolics is their antioxidant capability toward free radicals normally produced in cell metabolism or in response to external factors. Free radicals can damage biomolecules such as lipids, nucleic acids, and proteins; cause cellular membranes peroxidation;^{34,35} and attract various inflammatory mediators.³⁶

Phenolic acids are phenols characterized by a carboxylic functionality. They contain two distinguishing constitutive carbon frameworks: the hydroxycinnamic and hydroxybenzoic structures. Hydroxycinnamic acids are more common than hydroxybenzoic ones and consist mainly of *p*-coumaric, sinapic, ferulic, and caffeic acids;¹⁵ the latter is thought to be the most abundant in the diet.³

Phenolic acids exist primarily as conjugates of sugars, polysaccharides, or organic acids, whereas the free forms are less frequently observed in nature. The quantitatively most important conjugate of caffeic acid is its ester with quinic acid, 5-caffeoquinic acid (also known as chlorogenic acid). High concentrations of phenolic acids are found in coffee, apples, citrus fruits and juices, and the bran of cereal grains.³ Caffeic acid seems to

Received: August 16, 2011

Published: November 08, 2011

Scheme 1. Structure of Caffeic Acid

contribute to color stability and protection against oxidation in the red wines.³⁷

Recent experimental evidence suggests caffeic acid to have a beneficial impact *in vivo*.^{38–40} Caffeic acid has biological and pharmacological properties, such as antiviral,⁴¹ antioxidant,⁴² anti-inflammatory,⁴³ anticarcinogenic,⁴⁴ and immunomodulatory activities.⁴⁵ In addition, it completely blocks the production of reactive oxygen species (ROS).⁴⁶

According to a recent research,⁴⁷ caffeic acid was a superior antioxidant compared with *p*-coumaric and ferulic acids in inhibiting LDL oxidation^{48,49} but also in quenching radicals⁵⁰ and singlet oxygen.

The molecular basis for the antioxidant properties of phenolic compounds is recognized in three main mechanisms, arising from the direct reaction with free radicals.^{51–54} Another indirect modus operandi comes from their ability to chelate free metals that are involved in reactions finally generating free radicals.^{55,56}

As primary antioxidants, polyphenols inactivate free radicals according to the hydrogen atom transfer (HAT; eq 1), to the radical adduct formation (RAF; eq 2), and to the single electron transfer (SET; eq 3) mechanisms. In mechanism 1, the antioxidant, ArOH, reacts with the free radical, R[•], by transferring to it a hydrogen atom, through homolytic rupture of the O–H bond:



The radical adduct formation (RAF) mechanism (2) provides for the formation of an adduct between the radical and the antioxidant:



The SET mechanism (3) provides for an electron to be donated to the R[•]:



The products of mechanisms 1, 2, and 3 (ArO[•], ArOH-R[•], and ArOH^{+\bullet}) are aromatic structures in which the odd electron, originated through the reaction with the free radical, has the possibility to be spread over the entire molecule, resulting in a significant radical stabilization.^{51–54}

On the basis of the reaction rate constants of polyphenols with several radicals and the stability of the polyphenol-derived radicals, the antioxidant capability of some of these compounds was evaluated. Among the hydroxycinnamates, caffeic acid (see scheme 1) presented high rate constants toward several types of oxidant species like ROO[•] ($1.5 \times 10^7 \text{ M}^{-1} \text{ s}^{-1}$),⁵⁷ O₂^{•-} ($0.96 \times 10^6 \text{ M}^{-1} \text{ s}^{-1}$), HO[•] ($3.24 \times 10^9 \text{ M}^{-1} \text{ s}^{-1}$),⁵⁸ and ¹O₂ ($5.1 \times 10^6 \text{ M}^{-1} \text{ s}^{-1}$).⁵⁹

The caffeic acid oligomers have been shown to be very effective scavengers of 2,2-diphenyl-1-picryl hydrazyl (DPPH) and superoxide anion radicals.^{60,61}

On the basis of what was previously mentioned, it is evident that further research studies are needed and would be useful to fully understand the antioxidant capability of phenolics and to individuate a feasible molecular mechanism through which these plant metabolites scavenge free radicals.

The aim of this work is to study the reactivity of caffeic acid toward the OH radical, accepted to be one of the most reactive among the ROSs, with a very short half-life (around 10^{-9} s) and high reactivity. Different mechanisms and all possible sites of reaction/attack have been examined. Thermodynamic and kinetic data have been collected to identify the main channels of reaction.

2. METHODS

Geometry optimization and frequency calculations were performed by means of density functional theory (DFT). The Becke exchange and Lee, Yang, and Parr correlation (B3LYP)^{62–65} and the M05-2X⁶⁶ functionals were chosen. The 6-31+G(d) basis set^{67–70} was used for the representation of the C, O, and H atoms.

The M05-2X functional has been recommended for applications in thermochemistry, kinetics, and noncovalent interactions by its developers,⁶⁶ and it has been also successfully used by independent authors.^{71–77} However, B3LYP still represents the most widely used DFT functional, so it is used in this study for purpose of comparison.

Vibrational frequencies were obtained at the M05-2X and B3LYP levels, in order to compute the zero point energy corrections and to determine the nature of all stationary points, as minima and saddle points.

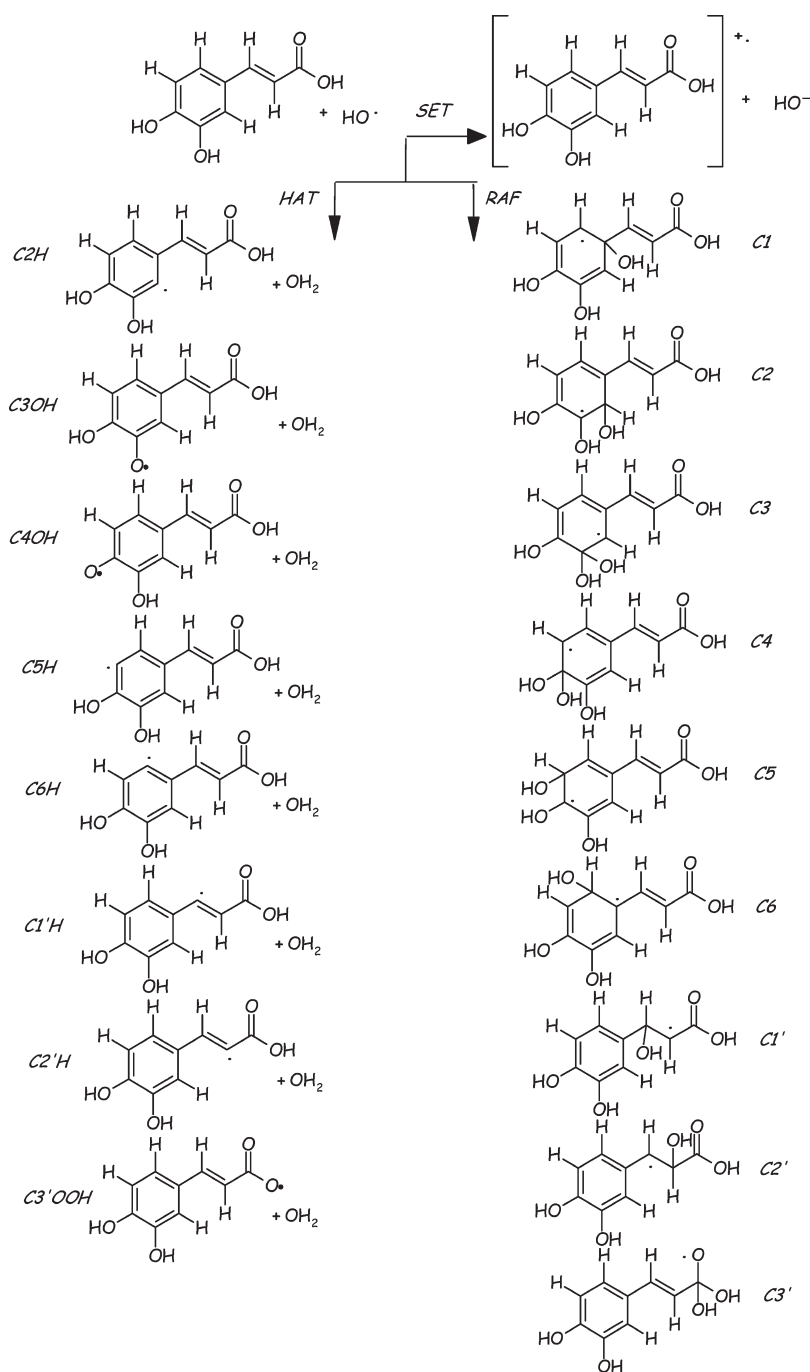
To confirm that a given transition state connects reactants and products and to carry out the dynamical computations, the intrinsic reaction coordinate (IRC) or minimum energy path (MEP)^{78,79} was constructed at the M05-2X level, starting from the respective saddle point geometry and going downhill to both the asymptotic reactant and the product channels, in an iso-inertial mass-weighted Cartesian coordinate system. A step size, δ_s , of 0.02 bohr (where s is the distance along the MEP which starts from 0 for the saddle point and assumes negative and positive values for reactants and products, respectively) was used in all cases. The second derivative matrix was computed at each of three points along the reaction path.

Solvent effects were introduced as single point computations on the optimized gas phase structures in the framework of the self-consistent reaction field polarizable continuum model (SCRF-C-PCM)^{80–82} in which the cavity is created *via* a series of overlapping spheres. The united atom topological model (UA0) applied on atomic radii of the UFF force field⁸³ was used to build the cavity, in the gas-phase equilibrium geometry. The dielectric constant values $\epsilon = 78.3553$ and $\epsilon = 2.2706$ were chosen to reproduce water and benzene media, respectively.

All rate constants were estimated by using canonical variational transition state theory (CVT),^{84–88} corrected by the semiclassical multidimensional small-curvature tunnelling (SCT) approach.^{89–92} The CVT/SCT method has been chosen since it has been successfully applied on the reactions of radical trapping performed by natural antioxidants.^{93–96}

All of the calculations were performed using the Gaussian 03⁹⁷ and Polyrate9.7⁹⁸ codes.

Scheme 2. Possible Reaction Mechanisms



3. RESULTS AND DISCUSSION

3.1. OH Scavenging by Caffeic Acid in the Neutral Form: Geometries and Energies. In Scheme 2, a representation of all possible reaction channels and attack sites for the trapping of the HO^\cdot by caffeic acid is shown.

Hydrogen atom transfer (HAT) can occur from the C_2H , C_3OH , C_4OH , C_5H , C_6H , $\text{C}_1'\text{H}$, $\text{C}_2'\text{H}$, and $\text{C}_3'\text{OOH}$ sites and radical adduct formation (RAF) at the C_1 , C_2 , C_3 , C_4 , C_5 , C_6 , C_1' , C_2' , and C_3' positions. In single electron transfer (SET), the one electron is transferred from the HOMO of the phenolic molecule to the hydroxyl radical.

In Tables 1 and 2, the relative energies of the stationary points (reactant complex (RC), transition state (TS), product complex (PC), and products (P) for the HAT and reactant complex (RC), transition state (TS), and product (P) for the RAF) with respect to the reactants (R) are reported for all mechanisms investigated, considering all positions of reactivity. In Figures 1, 2, 3, 4 and 5, the M05-2X and B3LYP optimized geometries for stationary points corresponding to the HAT, RAF, and SET mechanisms are shown.

Caffeic acid is a planar species, at both the M05-2X and B3LYP levels, characterized by electronic conjugation and delocalization that concern the whole molecule up to the carboxylic moiety.

Table 1. M052X/6-31+G(d) and B3LYP/6-31+G(d) Relative Energies (in kcal/mol) of the Stationary Points for the HAT Mechanism, Considering Both the Neutral and the Deprotonated (In Parentheses) Forms of Caffeic Acid

HAT M052X				
site	RC	TS	PC	P
C ₂ H	-6.57 (2.13)	7.56 (19.0)	-4.31 (3.38)	1.63 (11.93)
C ₅ H	-7.32 (/)	4.38 (/)	-10.56 (/)	0.32 (/)
C ₆ H	-4.66 (-9.96)	8.70 (19.0)	-3.14 (-4.54)	1.01 (11.93)
C _{1'} H	-8.92 (-9.92)	3.62 (2.89)	-14.12 (-17.32)	-5.70 (0.24)
C _{2'} H	-5.85 (-9.92)	7.19 (3.51)	-5.98 (-13.09)	-0.20 (0.24)
C ₃ OH	-5.96 (/)	3.03 (/)	-47.03 (-43.93)	-35.42 (-32.52)
C ₄ OH	-5.79 (/)	-1.00 (/)	-45.89 (-49.01)	-37.84 (-39.08)
C _{3'} OOH	-10.86 (/)	0.24 (/)	2.45 (/)	-2.50 (/)

HAT B3LYP				
site	RC	TS	PC	P
C ₂ H	-5.53 (-8.93)	5.52 (3.84)	3.77 (-7.69)	0.62 (0.02)
C ₅ H	-1.72 (/)	1.41 (/)	-10.13 (/)	-0.66 (/)
C ₆ H	-4.96 (-19.72)	5.80 (0.75)	-9.88 (-15.75)	6.27 (-0.55)
C _{1'} H	-8.09 (-19.67)	0.85 (-10.43)	-14.21 (-28.39)	-7.81 (-13.04)
C _{2'} H	-5.14 (-20.11)	4.00 (-11.36)	-6.13 (-24.67)	-2.16 (-9.93)
C ₃ OH	/ (/)	/ (/)	-49.79 (-59.99)	-39.35 (-49.17)
C ₄ OH	/ (/)	/ (/)	-48.78 (-66.29)	-42.09 (-56.21)
C _{3'} OOH	-9.92 (/)	-5.39 (/)	-14.92 (/)	-10.47 (/)

Table 2. M052X/6-31+G(d) and B3LYP/6-31+G(d) Relative Energies (in kcal/mol) of the Stationary Points for the RAF Mechanism, Considering Both the Neutral and the Deprotonated (In Parentheses) Forms of Caffeic Acid

RAF M052X			
site	RC	TS	P
C ₁	-1.06 (-9.96)	1.64 (12.30)	-16.20 (-8.31)
C ₂	-4.48 (-9.91)	-2.35 (5.09)	-26.64 (-18.35)
C ₃	-4.42 (-1.51)	-1.59 (5.58)	-24.76 (-15.90)
C ₄	-7.35 (/)	-5.99 (/)	-34.49 (-27.62)
C ₅	-7.36 (-9.84)	-4.24 (0.54)	-24.16 (-16.80)
C ₆	-4.69 (-9.83)	-2.41 (4.04)	-24.42 (-17.91)
C _{1'}	-4.80 (-9.96)	-3.41 (-2.87)	-35.41 (-35.05)
C _{2'}	-8.92 (-9.84)	-3.29 (-3.10)	-36.48 (-43.00)
C _{3'}	-10.88 (-10.50)	9.33 (18.38)	-4.63 (3.01)

RAF B3LYP			
site	RC	TS	P
C ₁	-5.13 (-19.72)	0.18 (-0.74)	-10.52 (-13.78)
C ₂	-4.28 (-19.70)	-4.27 (-8.48)	-22.77 (-25.36)
C ₃	/ (-13.28)	/ (-8.43)	-19.35 (-21.25)
C ₄	/ (/)	/ (/)	-29.06 (-33.40)
C ₅	-6.63 (-19.71)	-5.98 (-14.39)	-20.37 (-23.83)
C ₆	-3.94 (-19.70)	-3.04 (-10.41)	-21.25 (-25.16)
C _{1'}	-8.04 (-19.72)	-4.92 (-15.07)	-28.38 (-39.53)
C _{2'}	-8.07 (-19.51)	-2.29 (-15.47)	-30.27 (-48.08)
C _{3'}	-9.92 (-20.62)	8.04 (6.23)	-4.33 (-8.04)

In the minimum energy structure, the 3OH and 4OH groups are arranged in such a way as to realize a hydrogen bond.

All HAT reactant complex (RC) stationary points are characterized by a significant hydrogen bond established between the [•]OH and the hydrogen present on the site where the abstraction should occur.

In the reactant complex RC arising from the reaction at the C₂H site, two H bonds are established between the hydroxyl radical and the C₂H and C₃OH moieties. [•]OH acts as donor in the case of the interaction with the C₃OH group (1.93 and 1.90 Å, at M05-2X and B3LYP level) and as an acceptor toward C₂H (2.67 and 3.10 Å, at the M05-2X and B3LYP levels). The reaction passes through a transition state (imaginary frequency at 1462 and 1549 cm⁻¹, considering the M05-2X and the B3LYP functionals) in which the hydrogen atom attached to the C₂ is being transferred to the hydroxyl radical (C₂H[•]OH and C₂[•]HOH critical distances are 1.22 and 1.26 (M05-2X) and 1.18 and 1.31 Å (B3LYP)). M05-2X and B3LYP product complexes (PC) show the water molecule hydrogen-bonded to the C₃OH group at 2.12 and 1.97 Å, respectively.

As far as HAT at the C₃OH site is concerned, the two functionals give very different results. Namely, M05-2X finds a stationary point along the potential energy profile corresponding to a complex between reactants (see Figure 1), characterized by two hydrogen bonds involving the [•]OH and the C₃OH (1.93 Å) and the C₄OH (1.98 Å) groups. Computations employing the B3LYP functional have yielded a stationary point in which the H transfer has occurred spontaneously without passing through a saddle point and providing the product complex between the water molecule and the caffeic acid radicalized at the C₃O[•]. This different behavior may be due to the already known bad treatment and description of nonbonded interactions by the B3LYP functional.⁹⁹ In the M05-2X transition state (3234*i* cm⁻¹) for the reaction at the C₃OH, the hydrogen atom is contemporaneously bonded to the C₃O and to the OH at 1.07 and 1.33 Å. In the product complex, the water molecule is hydrogen-bonded

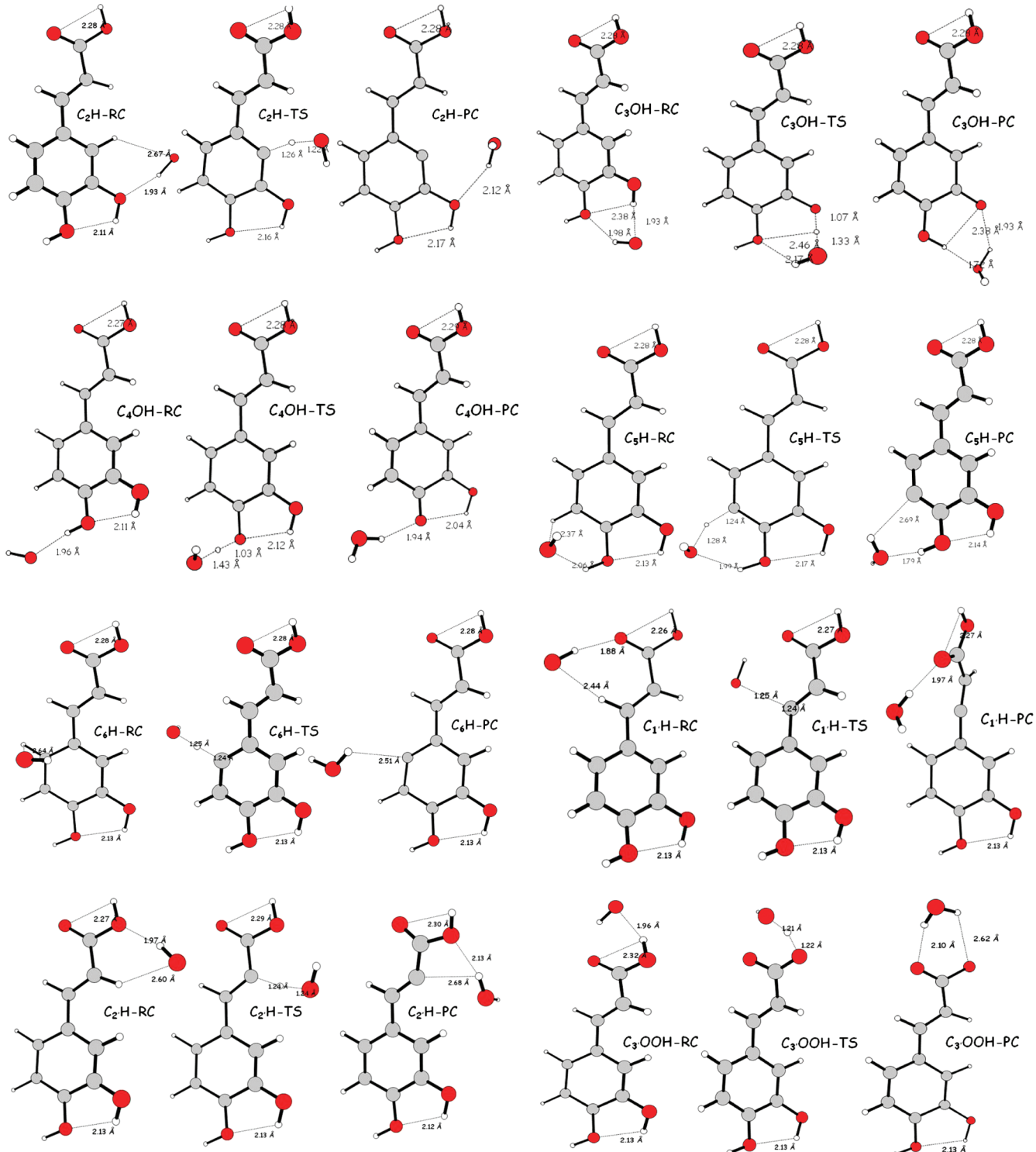


Figure 1. M05-2X optimized geometries of the stationary points encountered along the HAT mechanism.

to the radicalized C_3O at 1.93 (M05-2X) and 1.86 (B3LYP) Å. A further H-bond involves the $\text{C}_3\text{O}^\bullet$ and the hydroxyl at the C_4 , which is always recognized to be the crucial feature ensuring stability to the formed radical.¹⁰⁰

Results concerning HAT at the C_4OH moiety entail similar considerations to those for the HAT at C_3OH . B3LYP fails in locating a stationary point corresponding to both the reactant complex and the transition state. The complex between reactants

is obtained at the M05-2X level when the ${}^{\bullet}\text{OH}$ radical approaches the caffeic acid C_4OH group at a distance of 1.96 Å (H-bond). The H atom is then transferred to the hydroxyl radical through the M05-2X transition state TS, at the imaginary frequency of 2785 cm^{-1} corresponding to the stretching of the $\text{C}_4\text{O} \cdots \text{H}$ and $\text{C}_4\text{OH} \cdots \text{OH}$ couple of bonds (distances are 1.03 and 1.43 Å). In the product complexes at both M05-2X and B3LYP, H_2O interacts with the radicalized oxygen in the caffeic acid,

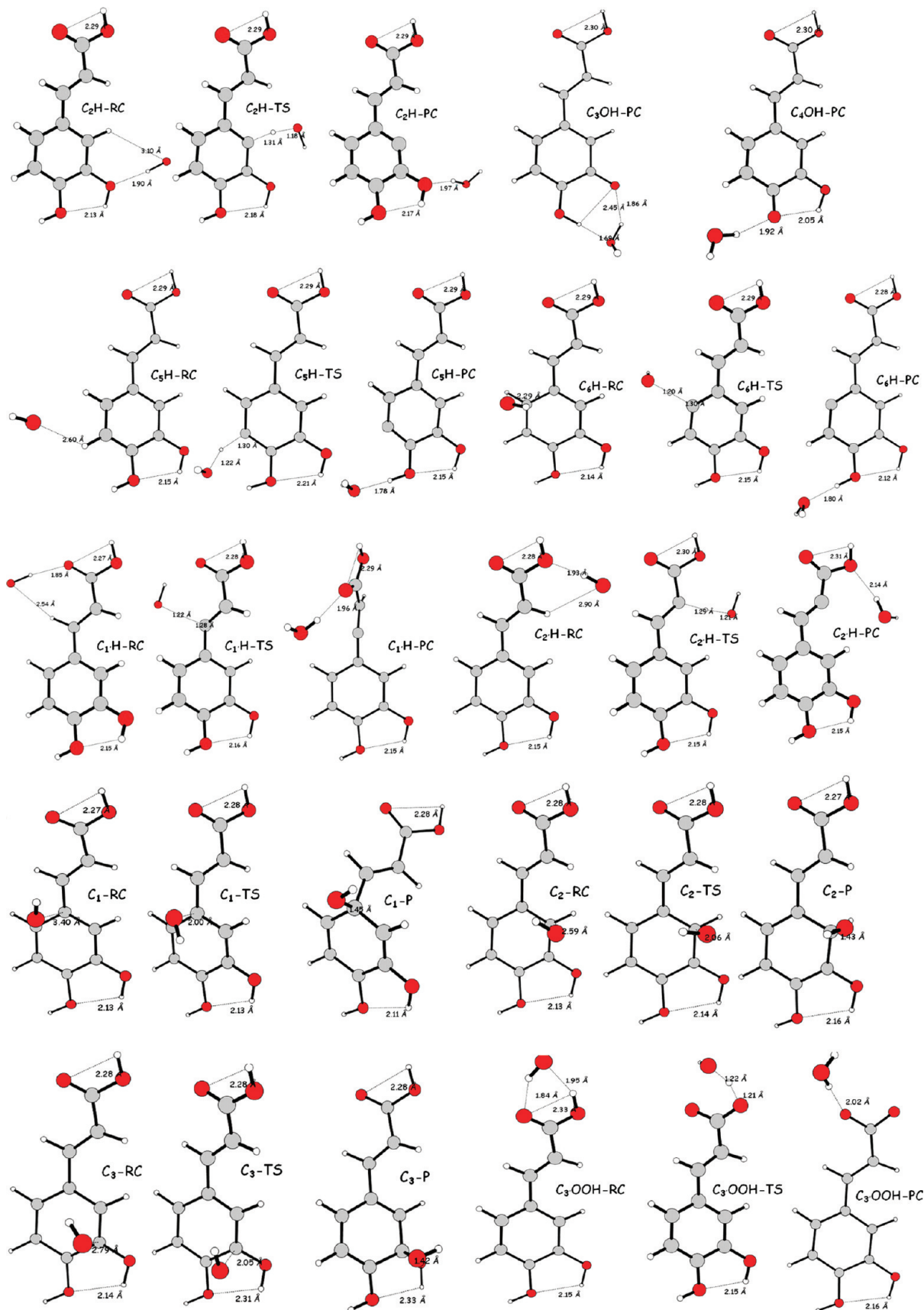


Figure 2. B3LYP optimized geometries of the stationary points encountered along the HAT mechanism.

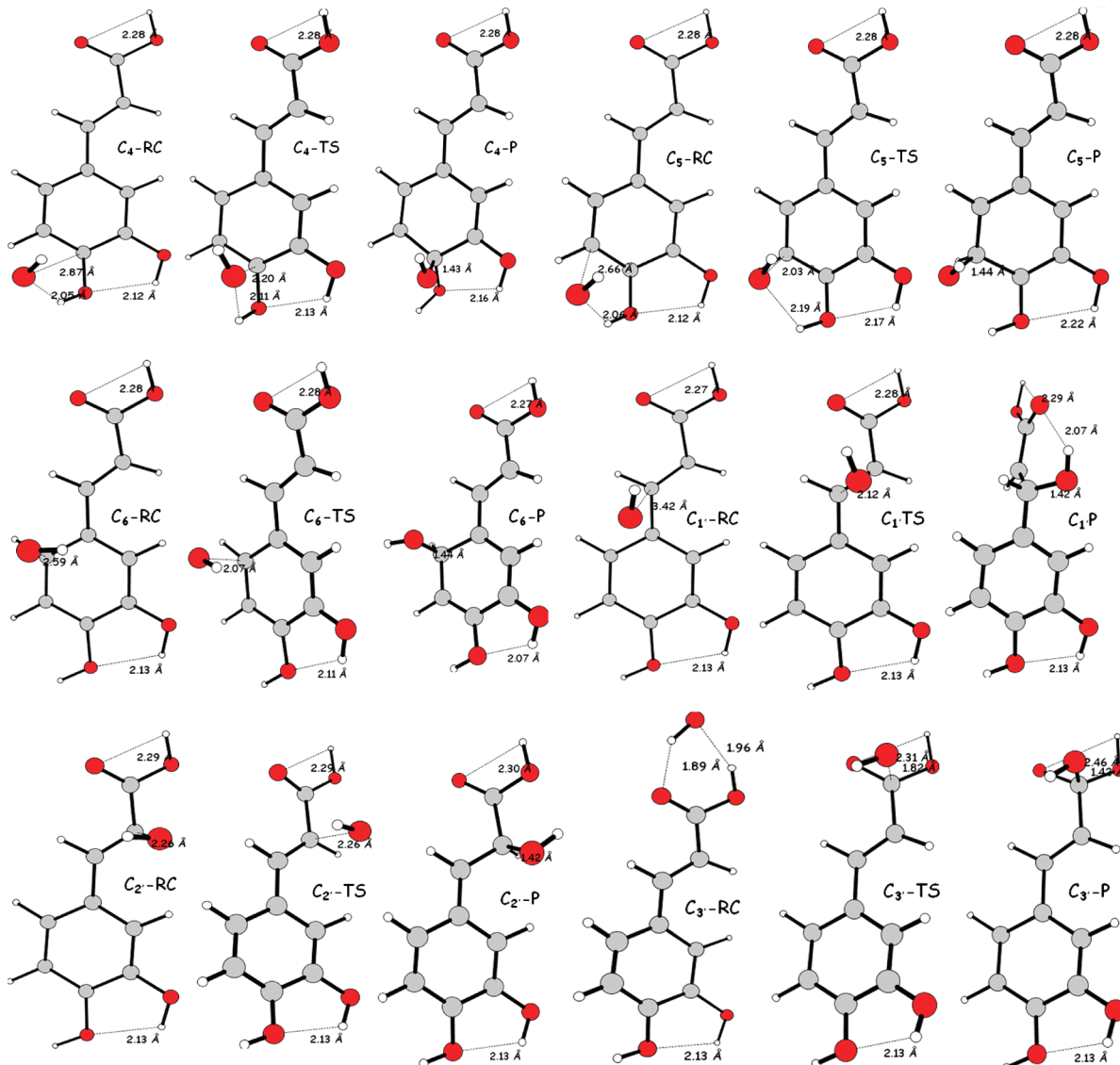


Figure 3. M05-2X optimized geometries of the stationary points encountered along the RAF mechanism.

establishing a H bond whose length is computed to be 1.94 and 1.92 Å for the two functionals, respectively. The internal hydrogen bond involving C₃OH and C₄OH is retained on going from RC to TS to PC, and it contributes to the stabilization of the electronic vacancy in the caffeic acid C₄O radical.

The hydrogen transfer process from the C₅H position starts with the formation of the reactant complex that is described differently by M05-2X and B3LYP functionals as far as the weak interactions are concerned. In the M05-2X minimized RC, *OH strongly interacts with the C₄OH group (2.06 Å) and to a lesser degree with the C₅H (2.37 Å). The RC within the B3LYP computations shows only a C₅H · · · OH hydrogen-like interaction (2.60 Å). The transition state for the H transfer is found when the C₅ · · · HOH and C₅H · · · OH distances assume the values of 1.24 and 1.28 Å (M05-2X) and 1.30 and 1.22 Å (B3LYP). Its nature of the saddle point is confirmed by the imaginary frequencies at 1524 and 1580 cm⁻¹, at the M05-2X and B3LYP levels, respectively. M05-2X and B3LYP geometries for the product complex are quite similar, as shown in Figures 1 and 2.

The reactant complex between *OH and caffeic acid at the C₆H moiety shows a hydrogen like interaction between the hydrogen in the hydroxyl radical and the π electrons in the aromatic ring of the phenolic molecule, at both levels of theory. Passing through the transition state in which the H atom is bonded to both the carbon atom at 1.24 and 1.30 Å, and to the hydroxyl radical at 1.25 and 1.20 Å, at M05-2X and B3LYP, respectively, the reaction proceeds toward the product complex. The M05-2X PC shows the water molecule interacting with the radicalized C₆ atom (HOH · · · C distance is 2.51 Å), while in the B3LYP computations the water molecule forms a H bond with the C₄OH group (see Figures 1 and 2).

The hydrogen atoms present in the C=C double bond may be in principle also abstracted by the OH radical, at both the C_{1'} and C_{2'} positions.

Because of the presence of the carboxylic group, the reactant complex (RC) within the pathway at the C₁H is characterized by a H bond with the carboxylic oxygen (1.88 and 1.85 Å, at the M05-2X and B3LYP levels, respectively). Abstraction of the C_{1'} bonded hydrogen atom occurs through the transition state

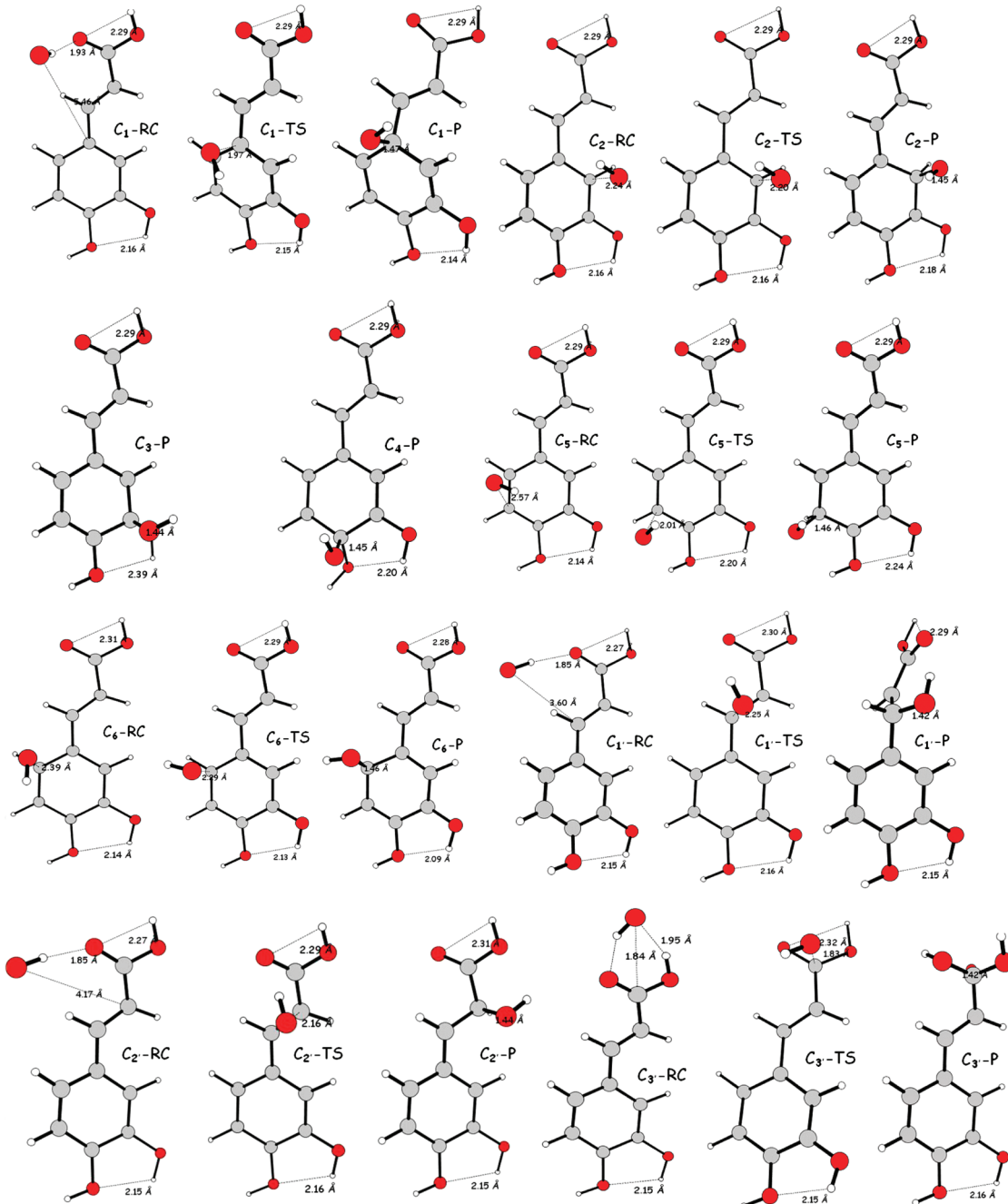


Figure 4. B3LYP optimized geometries of the stationary points encountered along the RAF mechanism.

(imaginary frequencies at 1605 and 1532 cm⁻¹, at the M05-2X and B3LYP levels, respectively) in which the critical distances C_{1'}···H and the C_{1'}H···OH assume the values of 1.24 and 1.25 Å (M05-2X) and 1.28 and 1.22 Å (B3LYP). The HAT C_{1'}H pathway product complex shows a H bond involving the water molecule and the carboxylic oxygen in the caffeic acid (~1.96 Å for both functionals) and a particular rearrangement of the ethylene group perpendicular to the plane of the ring for both functionals employed (see Figures 1 and 2). This reorganization should favor resonance and conjugation effects and thus a better stabilization of the unpaired electron in the just formed radical.

The RC for the HAT C_{2'}H reaction shows, like the HAT C_{1'}H one, a strong interaction between the OH radical and the

carboxylic group (see Figures 1 and 2). The H atom is shared between the C_{2'} and the O atoms in the transition state, for which animation of the vibrational modes at 1527*i* and 1513*i* cm⁻¹ frequency values proposes the stretching of the C_{2'}···H and C_{2'}H···OH bonds. M05-2X and B3LYP product complexes show the same geometrical features (see Figures 1 and 2).

As far as the H abstraction by ·OH from the COOH moiety is concerned, the reactant complex appears to be characterized by two strong H bonds in the reaction part, as shown in Figures 1 and 2, by both employed functionals, which predict also very similar geometries for the saddle point (imaginary frequencies are 1362 and 1372 cm⁻¹, at the M05-2X and B3LYP levels). To the contrary, the structure for the product complex is quite

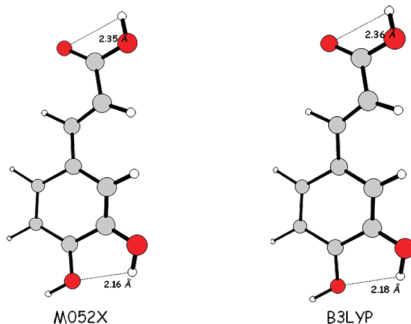


Figure 5. M05-2X and B3LYP optimized geometries of the radical cation arising from the SET mechanism.

different since the M05-2X optimized geometry shows the water molecule involved in two H bonds with the COO^* group (2.10 and 2.62 Å), while B3LYP computations locate on the potential energy profile a stationary point with only one H bond (2.02 Å).

The formation of the reactant complex is predicted to be energetically favored for all reaction sites by both functionals employed (see Table 1), especially in the case of the COOH ($\Delta E = -10.86$ and -9.92 kcal/mol with respect to the unbound reactants, at M05-2X and B3LYP, respectively). M05-2X and B3LYP also give the same trend of relative energetic stability, with the only exception being the C_5H RC, which is found to lie 7.32 (M05-2X) and 1.72 (B3LYP) kcal/mol below the asymptote. This difference in the energy is due to the diverse geometrical structure for this stationary point.

Energy barriers (TS relative energies reported in Table 1) for the H transfer, determined at the M05-2X level, indicate that this process is particularly favored from the C_4OH site, followed by the reaction at C_3OOH and C_3OH . In the case of the B3LYP computations, the lack of some stationary points not located on the potential energy profile prevents us from indicating an accurate trend.

HAT processes are predicted to be thermodynamically very favored in the case of the C_3OH and C_4OH groups, as the relative energies for the PC and P stationary points suggest.

In agreement with previous works,^{52–54,96,100} results reported here indicate that the C_4OH site seems to be the most reactive one within the HAT mechanism. The better reactivity of the C_4OH group toward the $\cdot\text{OH}$ is mainly due to the stability generated by the intramolecular H bond between the two phenolic groups that is retained on going from free caffeic acid to the reactant complex, to the transition state up to the product complex and free products. This H bond helps in stabilizing the electronic deficiency generated on the phenolic oxygen during the H abstraction reaction. Additionally, in the product complex and free products coming from radicalization at the 4OH site, the unpaired electron generated is delocalized over the whole molecule thanks to the electronic conjugation characterizing the caffeic acid. Atomic spin densities for the PC of the reaction channels listed in Table S1 in the Supporting Information indicate that when OH radicalization occurs at the C_4OH position, a broad delocalization of the unpaired electron involving the C_1 , C_2 , C_3 , C_5 , C_6 , $\text{C}_{1'}$, $\text{C}_{2'}$, and C_4O atoms occurs. Radicalization at the C_3OH entails a delocalization of the odd electron only on the aromatic ring since $\text{C}_{1'}$ and $\text{C}_{2'}$ atoms are not involved. For the other positions, this stability cannot be achieved.

The addition of the $\cdot\text{OH}$ radical to the carbon atoms in the caffeic acid (RAF mechanism) starts again with the formation of

weak-bonded complexes in which the radical is involved in hydrogen like interactions and/or interactions with the π electrons.

The reactant complex for the RAF process at the C_1 position is characterized by an interaction of the $\cdot\text{OH}$ with the π electrons and by a H bond with the carboxylic group, as far as M05-2X and B3LYP computations are concerned. The visualization of the imaginary frequencies for the transition state (at 497 (M05-2X) and 352 (B3LYP) cm^{-1}) shows the stretching of the $\text{HO}\cdots\text{C}_1$ incoming bond. In both cases, the $-\text{CH}=\text{CH}-\text{COOH}$ chain is slightly twisted with respect to the phenyl ring (the $\text{C}_2-\text{C}_1-\text{C}_{1'}-\text{C}_{2'}$ dihedral is found to be 18.43° and 15.56° , at the M05-2X and B3LYP levels, respectively). Finally, the product is characterized by a $\text{HO}-\text{C}_1\sigma$ bond at 1.45 and 1.47 Å; the conjugation between the $-\text{CH}=\text{CH}-\text{COOH}$ chain and the phenyl ring has completely disappeared (see Figures 3 and 4).

Both M05-2X and B3LYP reactant complexes (RC) present a weak interaction between the aromatic ring and the $\cdot\text{OH}$ ($\text{HO}\cdots\text{C}_2$ distance is 2.59 and 2.24 Å). The transition state is located when the $\text{HO}\cdots\text{C}_2$ distance assumes the value of 2.06 (at 428i cm^{-1}) and 2.20 (66i cm^{-1}) Å, considering the M05-2X and B3LYP computations. In the product, the HO that is now bonded to the C_2 at 1.43 (M05-2X) and 1.45 (B3LYP) Å is oriented in such a way as to realize an interaction of the hydrogen with the π electrons in the phenyl ring rather than a H bond with the hydroxyl attached at the C_3 .

Any attempt to locate the corresponding C_3 reactant complex within the RAF mechanism at the B3LYP level invariably led to structures that correspond to the final product for this channel or to the C_3OH HAT PC point. Only M05-2X locates a reactant complex on the potential energy profile, showing a $\text{HO}\cdots\text{C}_3$ distance of 2.79 Å and an interaction of the hydroxyl hydrogen with the π electrons (see Figure 3). In the M05-2X C_3 RAF transition state, the $\text{HO}\cdots\text{C}_3$ bond is forming at 2.05 Å, as indicated by the imaginary frequency at 403 cm^{-1} corresponding to the stretching of this bond. M05-2X and B3LYP product structures are shown in Figures 3 and 4 and present very similar arrangements.

Concerning the RAF at the C_4 position, again B3LYP does not find any structure corresponding to a reactant complex (as well as later to the transition state). This structure, indeed located with the M05-2X calculations for a $\text{HO}\cdots\text{C}_4$ distance of 2.87 Å, presents also a H bond with the C_4 hydroxyl. The C_4 RAF channel passes through a transition state in which the $\text{HO}\cdots\text{C}_4$ bond is forming at 2.20 Å (imaginary frequency at 247 cm^{-1}). OH finally establishes a σ bond with the C_4 carbon atom (distances are 1.43 and 1.45 Å, at M05-2X and B3LYP, respectively).

The reactant complex for the RAF at the C_5 position is very similar to the RC obtained for the RAF C_4 channel at the M05-2X level, while B3LYP computations find a stationary point in which the hydroxyl radical establishes a $\text{OH}\cdots\pi$ electron interaction (see Figures 3 and 4). The attack by the $\cdot\text{OH}$ radical on the C_5 carbon atom occurs when the $\text{HO}\cdots\text{C}_5$ distance assumes the critical value of 2.03 (M05-2X) and 2.01 (B3LYP) Å. The nature of the transition state for this saddle point is clearly indicated by the imaginary frequency at 391 and 282 cm^{-1} , at the M05-2X and B3LYP levels, respectively. The TS evolves into the product, in which the C_5-OH bond is completely formed at 1.44 and 1.46 Å.

The RC obtained for the RAF C_6 channel shows a weak interaction between the $\cdot\text{OH}$ and the C_6 carbon atom at 2.59 (M05-2X) and 2.39 (B3LYP) Å. In the transition state, the bond

$\text{OH}\cdots\text{C}_6$ measures 2.07 and 2.29 Å, at the M05-2X and B3LYP levels, respectively. The vibrational normal mode with an imaginary frequency at 435 and 207 cm^{-1} is the stretching of this bond. After the TS, a covalent product is located on the M05-2X and B3LYP potential energy profiles for a $\text{HO}-\text{C}_6$ bond of 1.44 and 1.46 Å, respectively. Only the C_6 carbon assumes the sp^3 configuration, while the other carbon atoms retain the sp^2 hybridization as it occurs for the other RAF channels (see Figures 3 and 4).

The process which leads to ${}^{\bullet}\text{OH}$ radical addition to the $\text{HC}=\text{CH}$ moiety (at positions $\text{C}_{1'}$ and $\text{C}_{2'}$) or to the carboxylic group may also occur. As far as the $\text{C}_{1'}$ addition is concerned, the reactant complex (RC) presents a different arrangement depending on the exchange-correlation functional used. Particularly, B3LYP optimization leads to a RC in which the OH radical establishes a H bond with the $-\text{COOH}$ group, while the M05-2X one shows a weak interaction between the hydroxyl radical and the $-\text{CH}=\text{CH}-$ moiety. ${}^{\bullet}\text{OH}$ addition occurs through the transition state TS for a $\text{HO}\cdots\text{C}_{1'}$ distance of 2.12 (M05-2X, 376*i* cm^{-1}) and 2.29 (B3LYP, 125*i* cm^{-1}) Å. The next point after the TS is the product whose geometry is predicted to be very similar by both functionals. The $\text{HO}-\text{C}_{1'}$ bond assumes the value of 1.42 Å in both cases, with the OH pointing toward the oxygen of the $-\text{COOH}$ group (H bond is 2.07 and 1.94 Å at the M05-2X and B3LYP levels, respectively).

${}^{\bullet}\text{OH}$ addition at the $\text{C}_{2'}$ position entails the formation of the reactant complex that, at both M05-2X and B3LYP levels of theory, is characterized by a strong H bond with the carboxylic group (see Figures 3 and 4). At the saddle point for radical addition, the $\text{HO}-\text{C}_{2'}$ distance is 2.26 Å at the M05-2X level and 2.16 Å at the B3LYP level (imaginary frequencies are 283 (M05-2X) and 183 (B3LYP) cm^{-1}). The $\text{HO}-\text{C}_{2'}$ bond is completely formed in the product at 1.42 (M05-2X) and 1.44 (B3LYP) Å.

In the ${}^{\bullet}\text{OH}$ addition at the $-\text{COOH}$ group, the radical approaches in the same plane of the molecule because of the formation of two H bonds with the carboxylic group (see Figures 3 and 4). The transition state sees the ${}^{\bullet}\text{OH}$ attacking the carboxylic carbon atom at 1.82 (M05-2X, 663*i* cm^{-1}) and 1.83 (B3LYP, 497*i* cm^{-1}) Å and leads to the product characterized by a $\text{HO}-\text{C}_{\text{COOH}}$ bond whose length is found to be 1.42 Å by both functionals.

In Table 2, the energies for the three regions RC, TS, and P relative to the free reactants taken into account within all channels for the RAF mechanism are reported.

Reactant complex formation is energetically favored in all investigated cases, by both M05-2X and B3LYP functionals, especially considering the addition at the $\text{C}_{3'}$ position in the side chain (-10.88 and -9.92 kcal/mol, at M05-2X and B3LYP level, respectively) because of the formation of several H bonds.

Energy barriers for the addition of the ${}^{\bullet}\text{OH}$ on the caffeic acid are found all below the asymptote, suggesting that this pathway occurs very easily. Exceptions to it are represented by the ${}^{\bullet}\text{OH}$ addition on the C_1 and C_3OOH positions for which TSs are computed to lie at 1.64 and 9.33 kcal/mol, at the M05-2X level, and 0.18 and 8.04 kcal/mol, at the B3LYP level, over the asymptote. This is quite expected since ${}^{\bullet}\text{OH}$ addition to the C_1 site entails the rupture of the π delocalization from the aromatic ring to the $-\text{CH}=\text{CH}-\text{COOH}$ chain and the rearrangement of the latter, while RAF at the C_3OOH destroys the delocalization involving the carboxylic group locating the unpaired electron to the oxygen in the carbonyl.

The final adducts are found to lie below the asymptote for all examined cases, indicating that the RAF process is quite

thermodynamically favored. The P's for the RAF $\text{C}_{1'}$ and RAF $\text{C}_{2'}$ are found at -35.41 and -36.48 kcal/mol, at the M05-2X level, and -28.38 and -30.27 kcal/mol, at the B3LYP level. In these adducts, the unpaired electron may be delocalized on the oxygen in the carbonyl in the case of RAF $\text{C}_{2'}$ and over the aromatic ring in the case of the RAF $\text{C}_{1'}$, as suggested by the atomic spin densities reported in Table S2 in the Supporting Information for the final adducts. P for the RAF C_4 is found at -34.49 (M05-2X) and -29.06 (B3LYP) kcal/mol. The odd electron may be delocalized over the aromatic ring and up to the $\text{C}_{1'}$ and $\text{C}_{2'}$ carbon atoms, even if no involvement of the carboxylic group is detected in this case (see atomic spin densities in Table S2). This significant possibility of delocalization of the unpaired electron in the final adduct, which does not occur for the RAF at the remaining positions, is the main feature of stabilization.

Considering both the thermodynamics and the kinetics of the process, the most reactive site within the RAF process is represented by the C_4 position. In fact, the lowest barrier corresponds to the radical addition to this site, as well as a good thermodynamic stabilization. This is mainly due to the broad electronic delocalization that occurs when ${}^{\bullet}\text{OH}$ adds to the C_4 carbon atom. However, the radical addition to all carbon atoms, with the only exception being the carbon in the $-\text{COOH}$ group, seems to be quite viable since all stationary points are predicted to lie below the entrance channel.

A single electron transfer (SET) process occurs without passing through a saddle point, so for this channel, information about the structure of the radical cation of caffeic acid upon single electron removal and reaction energy (ΔE) for the process are provided.

The caffeic acid radical cation is a planar species as the parent molecule, at both the M05-2X and B3LYP levels. H bonds are retained upon electron removal (Figure 5). Analysis of the atomic spin densities (Table S3 in the Supporting Information) reveals that the unpaired electron is delocalized over the aromatic ring, with the exception of the C_5 carbon atom, and also on the $-\text{CH}=\text{CH}-\text{COOH}$ chain, especially involving $\text{C}_{1'}$ and $\text{C}_{2'}$.

The ΔE of reaction for the SET process is computed to be 149.38 and 140.22 kcal/mol, at the M05-2X and B3LYP levels, so it is found to be endergonic by both functionals. So, this mechanism may be ruled out for the possible radical scavenging activity of caffeic acid toward the hydroxyl radical with respect to HAT and RAF pathways.

Concerning the performance of the two exchange-correlation functionals for the prediction of the three mechanisms, we may point out that both give shapes for the classical reaction profiles that are qualitatively similar. But, they differ considerably in the values for the relative energies. In particular, B3LYP underestimates the barrier heights with respect to M05-2X. In some cases, B3LYP fails in locating RC and TS on the potential energy profile (C_3OH and C_4OH HAT, and C_3 and C_4 RAF). This behavior is mainly ascribed to its development since it has only been parametrized against a data set of thermochemistry, so its tendency toward predicting lower barrier heights is shown.¹⁰¹ Indeed, M05-2X has been parametrized and tested also against 38 barrier heights for hydrogen transfer (HT) processes, 18 of which involve radicals as reactants and products, and it is recommended by the authors to be used for thermochemical kinetics, noncovalent interactions (especially weak interaction, hydrogen bonding, $\pi-\pi$ stacking, and interactions energies of nucleobases), giving the best composite results for energetics.⁶⁶

Table 3. M05-2X/6-31+G(d) Activation (ΔE^\pm) and Reaction (ΔE) Energies (in kcal/mol) in Water and Benzene Media

	ΔE^\pm		ΔE	
	water	benzene	water	benzene
	SET			
/	/		25.94	79.90
	HAT			
C ₂	7.57	6.78	-0.65	0.57
C ₅	6.47	4.75	-0.84	-0.39
C ₆	8.90	8.65	-1.08	-0.03
C _{1'}	4.47	3.35	-7.83	-6.43
C _{2'}	7.29	6.80	-2.18	-1.08
C ₃ OH	4.37	1.82	-36.20	-35.96
C ₄ OH	-0.85	0.30	-38.44	-38.30
C _{3'} OOH	0.95	0.24	-4.13	-3.28
	RAF			
C ₁	0.13	1.08	-16.40	-16.36
C ₂	-3.15	-2.63	-27.09	-23.99
C ₃	-2.00	-1.79	-25.44	-25.30
C ₄	-3.89	-4.74	-32.84	-34.13
C ₅	-1.55	-3.39	-22.03	-23.75
C ₆	-2.52	-2.39	-26.13	-25.38
C _{1'}	-2.99	-3.29	-34.31	-35.25
C _{2'}	-4.41	-4.58	-36.65	-36.92
C _{3'} OOH	10.56	9.54	-3.59	-4.56

Furthermore, it has been shown elsewhere¹⁰² that functionals that perform well for hydrogen-transfer barrier heights also perform well for barrier heights of more general classes of reaction.

Considering these arguments and also that M05-2X functionals have been successfully used by independent authors,^{71,74,77} we believe that the energetics predicted by M05-2X may be more reliable.

In Table 3, the activation (ΔE^\pm) and reaction (ΔE) energies are listed for all HAT, RAF, and SET mechanisms, in both polar (water) and nonpolar (benzene) media, to observe the effects of the environment on the energetics and thus on the viability of the three mechanisms investigated. The results are reported only with the M052X functional because of its better reliability, as discussed previously.

The channel requiring the lower activation energy within the HAT mechanism is the C₄OH one in a water medium (-0.85 kcal/mol), while in a benzene medium the C₃'OOH HAT presents the lowest barrier height (0.24 kcal/mol), even if C₄OH HAT follows with a barrier of 0.30 kcal/mol.

As far as the RAF process is concerned, the reactivity order in terms of activation energy in a water medium is C_{2'} (-4.41 kcal/mol) > C₄ (-3.89 kcal/mol) > C₂ (-3.15 kcal/mol) > C_{1'} (-2.99 kcal/mol) > C₆ (-2.52 kcal/mol) > C₃ (-2.00 kcal/mol) > C₅ (-1.55 kcal/mol) > C₁ (0.13 kcal/mol) > C_{3'} (10.56 kcal/mol). In a benzene medium, the order found is C₄ (-4.74 kcal/mol) > C_{2'} (-4.58 kcal/mol) > C₅ (-3.39 kcal/mol) > C_{1'} (-3.29 kcal/mol) > C₂ (-2.63 kcal/mol) > C₆ (2.39 kcal/mol) > C₁ (1.08 kcal/mol) > C_{3'} (9.54 kcal/mol). So, the medium does not seem to influence the barrier height or the reactivity order.

Also, the thermodynamics seem to be insensitive to both polar and nonpolar media since reaction energies are more or less the same computed in the gas phase. Again, HAT at the C₄OH and RAF at the C₄ positions are the more reliable pathways.

The SET pathway is likely to be favored by polar environments that may solvate the ionic species formed during the reaction, so the ΔE of the reaction in solution could provide a more complete investigation. In water and benzene, the ΔE values of reaction reported in Table 3 are quite affected by the solvent, and in particular, a water medium lowers the value by around 125 kcal/mol. The effect of a nonpolar environment is also quite important since the ΔE of reaction decreases by ~70 kcal/mol. However, the SET process remains to be thermodynamically unfavored with respect to HAT and RAF, also taking into account the solvent, so that it may be ruled out for the possible radical scavenging activity of caffeic acid toward the hydroxyl radical.

On the basis of these results, the HAT and RAF mechanisms are found to be very feasible as possible channels for the scavenging activity of the caffeic acid toward the hydroxyl radical. In the case of the former, the channel exhibiting the more reliable energetics is the hydrogen abstraction from the hydroxyl attached at the C₄. The RAF process indeed provides very low activation energies and thermodynamical feasibility regardless of the particular site of addition, with a slight preference for the insertion at the C₄ position. The presence of the environment and its polarity do not seem to particularly influence the energetics involved.

3.2. OH Scavenging by Caffeic Acid in the Deprotonated form. The pK_a of caffeic acid is 4.62,⁵⁸ indicating that this compound will primarily exist in anion form in the carboxylic functionality in the environment at physiological pH. So, to provide a detailed exploration about the radical scavenging activity of caffeic acid toward $^{\bullet}\text{OH}$, also the anionic form of caffeic acid has been taken into account, considering HAT, RAF, and SET mechanisms.

The anion of the caffeic acid is also a planar species, at both the M05-2X and B3LYP levels.

Concerning the HAT mechanism, the RC stationary points are characterized by the formation of strong H bonds involving the $^{\bullet}\text{OH}$ radical and the carboxylate group of the caffeic acid. The only exception is the HAT at the C₂H position, in which the hydrogen-like interaction is established with the 3OH group at both the M05-2X and B3LYP levels (see Figures S1 and S2 in the Supporting Information). HAT at the C₂H proceeds toward the transition state, in which the H is shared between the OH radical (C₂H ··· OH distance is 1.24 and 1.20 Å) and the carbon atom (C₂ ··· HOH distance is 1.25 and 1.35 Å), leading to the product complex (see Figures S1 and S2).

Both functionals fail in locating, on the potential energy profile, the reactant complex coming from the interaction between the $^{\bullet}\text{OH}$ and the hydrogen attached to the C₅, C₃OH, and C₄OH positions. Concerning the two latter cases, the optimizations yield as final results the product complex for the HAT C₃OH and HAT C₄OH, respectively. In the former, indeed, M05-2X and B3LYP computations yield the product complex PC referable to the HAT C₄OH; i.e., no stationary points (RC, TS, PC, and thus P) for the HAT C₅ are found, so this channel is ruled out.

HAT at the C₆H site starts with the formation of a reactant complex characterized by a strong H bond (1.63 Å at both M05-2X and B3LYP) between the hydroxyl radical and one oxygen atom of the carboxylate. Through a transition state

(1511*i* (M05-2X) and 1630*i* (B3LYP) cm^{-1}) in which the hydrogen is contemporaneously bonded to both the C_6 atom (1.23 (M05-2X) and 1.33 (B3LYP) Å) and the $^{\bullet}\text{OH}$ group (1.27 (M05-2X) and 1.20 (B3LYP) Å), it is transferred to the hydroxyl radical forming the product complex between the H_2O and the C_6 radicalized caffeic acid.

The H-atom transfer reaction occurring between the $^{\bullet}\text{OH}$ radical and the $\text{C}_1'\text{H}$ sees the formation of a reactant complex obtained for a $\text{C}_1'\text{H}\cdots\text{OH}$ distance of 1.63 Å at both levels of theory. The transition state, necessary to proceed toward the product complex, is characterized by a $\text{C}_1'\cdots\text{HOH}$ and a $\text{C}_1'\text{H}\cdots\text{OH}$ distance of 1.24 and 1.25 Å at the M05-2X (imaginary frequency is 1498 cm^{-1}) level and 1.29 and 1.21 Å at the B3LYP level (imaginary frequency is 1534 cm^{-1}). Both M05-2X and B3LYP product complexes predict the delocalization of the unpaired electron on the whole molecule with the exception of the carboxylate, which is quite perpendicular to the rest of the molecule (see Figures S1 and S2, Supporting Information).

For the HAT process at the C_2H position, the reactant complex shows a H bond established between the hydroxyl radical and the carboxylate group (1.60 and 1.62 Å, at M05-2X and B3LYP, respectively). Both M05-2X and B3LYP saddle points (imaginary frequencies are 1624 and 1159 cm^{-1}) for the H-transfer show the incoming bond of the hydrogen to the $^{\bullet}\text{OH}$ ($\text{C}_2'\cdots\text{H}$ and $\text{C}_2\text{H}\cdots\text{OH}$ distances are 1.21 and 1.31 Å and 1.25 and 1.29 Å, at the M05-2X and B3LYP levels, respectively). In the product complex, the conjugation between the $-\text{CH}=\text{CH}-\text{COO}^-$ and the aromatic ring is lost, especially as far as the B3LYP computations are concerned ($\text{O}-\text{C}_3'-\text{C}_2'-\text{C}_1'$ dihedral is 38.81°).

Product complexes for the C_3OH and C_4OH HAT show the water molecule hydrogen bonded to the radicalized oxygen atom in the caffeic acid. B3LYP indicates that the carboxylate group is not coplanar with the rest of the molecule, as can be noted from Figures S1 and S2 (Supporting Information).

With regard to the energetics of the HAT process for the anion of the caffeic acid (values in parentheses in Table 1), we may conclude again that the hydrogen attached to the C_4 carbon atom is the most susceptible to be transferred to the hydroxyl radical, in such a way that the computations do not find a complex between reactants, and the thermodynamics are particularly favored in this case.

As expected, B3LYP underestimates barrier heights and overestimates thermodynamics of all channels of the HAT process with respect to the M05-2X.

RAF at the C_1 starts with the formation of the reactant complex that again is characterized by the establishment of a H bond between the hydroxyl radical and the carboxylate group, as occurred for the HAT at the C_6 , C_1' , and C_2' and as it will occur for the RAF at the C_2 , C_5 , C_6 , C_1' , and C_2' . In the saddle point for the $^{\bullet}\text{OH}$ addition, whose nature of transition state is confirmed by the imaginary frequencies at 434 and 331 cm^{-1} , at the M05-2X and B3LYP levels, respectively, the distance $\text{HO}\cdots\text{C}_1$ assumes the values of 2.04 Å (M05-2X) and 2.00 Å (B3LYP). The final adduct shows a $\text{HO}-\text{C}$ σ bond and the disappearance of the conjugation between the $-\text{CH}=\text{CH}-\text{COO}^-$ and the phenyl (see Figures S3 and S4 in the Supporting Information).

After the formation of the reactant complex, the RAF process at C_2 proceeds toward the final adduct after passing through the transition state (434*i* (M05-2X) and 236*i* (B3LYP) cm^{-1}) in which the $^{\bullet}\text{OH}$ is approaching the C_2 carbon atom at 2.07 and 2.10 Å, at the M05-2X and B3LYP levels, respectively.

The reactant complex for the RAF C_3 presents a $^{\bullet}\text{OH}$ radical pointing toward the carbon atom at a distance of 2.89 and 2.97 Å, which becomes 2.08 and 2.00 Å in the saddle point (imaginary frequencies are 279 and 334 cm^{-1}), and 1.43 and 1.45 Å in the final adduct, at the M05-2X and B3LYP levels, respectively.

Both M05-2X and B3LYP computations fail in locating the reactant complex for the RAF at C_4 , since optimizations yield the final adduct at C_4 for a $\text{HO}-\text{C}_4$ distance of 1.45 and 1.47 Å, respectively. The B3LYP final adduct presents a loss of conjugation between the side chain and the rest of the molecule with respect to the M05-2X one.

$^{\bullet}\text{OH}$ addition at the C_5 site occurs through a saddle point in which the radical approaches the carbon at 2.11 Å with an imaginary frequency of 185 cm^{-1} , as indicated by the M05-2X computations, and 1.94 Å with an imaginary frequency of 342 cm^{-1} considering the B3LYP ones. The $\text{HO}-\text{C}_5$ bond is finally established in the final adduct at 1.46 and 1.48 Å, as far as M05-2X and B3LYP optimizations are concerned.

Upon the formation of the reactant complex, the RAF process at C_6 evolves toward the transition state in which the $\text{HO}\cdots\text{C}_6$ bond distances are 2.11 and 2.23 Å and the imaginary frequencies are 376 and 250 cm^{-1} , at the M05-2X and B3LYP levels, respectively. In the next product of the reaction, the $\text{HO}-\text{C}_6$ bond length is 1.45 (M05-2X) and 1.47 (B3LYP) Å.

RAF at C_1' and C_2' entails the formation of the reactant complex characterized by a H bond with the negative carboxylate group in both cases. The transition state for the hydroxyl radical addition occurs for a $\text{HO}\cdots\text{C}_1'$ and $\text{HO}\cdots\text{C}_2'$ distance of 2.11 and 2.18 Å, at the M05-2X level, and 2.16 and 2.36 Å, at the B3LYP one. The nature of the TS is confirmed by the imaginary frequencies at 410 (M05-2X) and 206 (B3LYP) cm^{-1} and 373 (M05-2X) and 140 (B3LYP) cm^{-1} , for the RAF C_1' and RAF C_2' , respectively. Geometries of the final adduct within RAF at C_1' and C_2' are predicted to be very similar by both M05-2X and B3LYP functionals (see Figures S3 and S4, Supporting Information).

Finally, the RAF process at the C_3' in the carboxylate entails the transition through the saddle point in which the hydroxyl radical is approaching the carbon atom at 1.77 and 1.71 Å, with an imaginary frequency of 436 and 509 cm^{-1} , at the M05-2X and B3LYP levels, respectively. The product shows the formation of a $\text{HO}-\text{C}_3'$ bond whose distance is 1.45 and 1.47 Å, as far as the M05-2X and B3LYP computations are concerned.

Formation of the reactant complexes is exothermic for all sites except for the C_3 one, because of the different arrangement of the adduct, as indicated before. Transition states are found at 12.30 (C_1), 5.09 (C_2), 5.58 (C_3), 0.54 (C_5), 4.04 (C_6), -2.87 (C_1'), -3.10 (C_2'), and 18.38 (C_3') kcal/mol with respect to the asymptote, and when compared to the values obtained for the neutral form of the caffeic acid they show a reduced reactivity toward the $^{\bullet}\text{OH}$ scavenging. Also, the thermodynamics of the process are less favored with respect to the neutral form of the antioxidant. Again, the C_4 site may be recognized as the most reactive in the radical adduct formation mechanism (the results in parentheses in Table 2).

The ΔE values of 57.50 (M05-2X) and 35.77 (B3LYP) kcal/mol for the single electron transfer (SET) process indicate that this mechanism is quite unfavored also when the antioxidant is present in the ionic form, and thus it can be concluded that caffeic acid does not follow this reaction channel.

3.3. Rate Constants. The M05-2X/6-31+G(d) computed rate constants as a function of the temperature for the H atom abstraction from the C_4OH group and for the radical addition at

Table 4. Rate Constants ($M^{-1} s^{-1}$) Computed at M052X Level of Theory for the HAT Mechanism at the 4OH Site of Caffeic Acid

T (K)	k_{TST}	k_{CVT}	$k_{CVT/SCT}$
150	3.82×10^{11}	1.25×10^{10}	1.22×10^{10}
200	5.64×10^{10}	4.57×10^9	4.35×10^9
300	9.76×10^9	1.85×10^9	1.65×10^9
400	4.65×10^9	1.31×10^9	1.12×10^9
500	3.31×10^9	1.07×10^9	9.33×10^8
600	2.85×10^9	1.06×10^9	9.39×10^8

Table 5. Rate Constants ($M^{-1} s^{-1}$) Computed at M052X Level of Theory for the RAF Mechanism at the C₄ Site of Caffeic Acid

T (K)	k_{TST}	k_{CVT}	$k_{CVT/SCT}$
150	1.26×10^{14}	1.26×10^{14}	1.25×10^{14}
200	3.20×10^{12}	2.90×10^{12}	2.16×10^{12}
300	9.33×10^{10}	7.29×10^{10}	6.00×10^{10}
400	1.84×10^{10}	1.33×10^{10}	1.15×10^{10}
500	7.59×10^9	5.29×10^9	4.70×10^9
600	4.55×10^9	3.06×10^9	2.78×10^9

the C₄ position in the caffeic acid by the HO[•] radical are collected in Tables 4 and 5. Our choice to report only the MEP at the M05-2X level is due to the fact that this functional provides more reliable kinetics and thermodynamics than B3LYP, also according to previous works on this matter.^{95,96}

Concerning the H-atom transfer mechanism, all rate constants (k_{TST} , k_{CVT} , and $k_{CVT/SCT}$) are on the order of 10^9 at 300 K (Table 4), meaning that the reaction is very fast and diffusion-limited, and underlining the excellent antioxidant activity of caffeic acid toward the HO[•] radical.

It is worth noting that important variational effects (i.e., the ratio between variational CVT and conventional TST rate constants) are present in the hydrogen abstraction reaction under investigation. The differences between the conventional transition-state rate constants (k_{TST}) and the variational transition-state rate constants (k_{CVT}) are caused by these marked variational effects, which are more evident at low values of temperature. At all temperatures, the variational transition state location, specified by the value of $s^*CVT(T)$, moves toward the reactant side of the PES. For example, the value of $s^*CVT(T)$ is found at -0.1355 bohr at 300 K.

As can be noted by the $k_{CVT/SCT}$ values reported in Table 4, and due to the little significant barrier height for the H abstraction from the C₄OH group, tunneling plays a rather modest role in the dynamics of the HAT process.

The computed rate constants for the RAF process (Table 5) indicate that this channel is slightly favored with respect to the former. In fact, at 300 K, the rate constants are on the order of 10^{10} .

In this case, variational effects on computed rate constants are less significant. At 300 K, k_{TST} and k_{CVT} values are 9.33×10^{10} and $7.29 \times 10^{10} M^{-1} s^{-1}$, indicating that the classical potential energy contribution predominates over the entropy contribution. Again, tunneling contributions on thermal rate constants are quite negligible, as expected since the addition reaction is a barrierless reaction and involves the movement of heavy atoms.

The calculated rate constants for both abstraction and addition reactions show a negative temperature dependence and, consequently, a negative activation energy, which may be expected for a free radical reaction involving HO[•] as the most reactive among the ROS species.

Pulse radiolytic experiments about the HO[•] scavenging capability of caffeic acid, conducted in slightly alkaline solutions,¹⁰³ have yielded rate constants of $7.4 \times 10^9 M^{-1} s^{-1}$. Other literature values^{104,105} are $5.5 \pm 0.8 \times 10^9 M^{-1} s^{-1}$ and $3.24 \times 10^9 M^{-1} s^{-1}$. Experimentally, the HAT mechanism is suggested to be the essential channel, followed by caffeic acid, and thus is responsible for these rate constants.¹⁰³ At 300 K, the theoretical rate constant computed by us for the abstraction reaction is on the same order of magnitude as the experimental values.

4. CONCLUSIONS

In this study, we have performed theoretical calculations to investigate the efficiency of a naturally occurring antioxidant molecule, i.e., the caffeic acid, in scavenging the very damaging HO[•] free radical, which can arise in living organisms.

Three different pathways of reaction have been deeply analyzed, H-atom abstraction, radical addition, and single electron transfer. All possible sites of reaction have been investigated in order to obtain the more reliable pathways.

Both hydrogen abstraction and radical addition channels are very feasible, in terms of thermodynamics and kinetics, in the gas phase and in polar and nonpolar media. Within the former mechanism, the most reactive site is the phenolic OH attached to the C₄ carbon in the aromatic ring, since a strong exothermicity (≈ 40 kcal/mol) and a negative barrier height (-1 kcal/mol) are obtained within this channel. HO[•] addition on the C₄ carbon atom is the favorite within radical addition formation. The single electron transfer process seems to be very unlikely since unfavorable thermodynamics are found for this mechanism, regardless of the presence on the environment.

The rate constants for the two most probable mechanisms were independently calculated by using variational transition-state theory with multidimensional tunneling. Obtained values are 1.8548×10^9 and $7.2868 \times 10^{10} M^{-1} s^{-1}$, for the hydrogen abstraction and radical addition, respectively. Variational effects are significant in the case of the hydrogen transfer process, due to the flat potential energy profile, so that conventional transition state theory does not seem to be adequate for this reaction.

Tunneling seems to have a negligible effect in both cases.

We have found that the HO[•] addition mechanism on caffeic acid is slightly favored with respect to the hydrogen transfer.

The final rate constants present a negative temperature dependence, leading to a negative activation energy. This negative value may be due to the negative value of the enthalpy associated with the generalized transition state, where the tunneling effect is negligible.

The agreement with available experimental data lends confidence to the theoretical level and model used.

■ ASSOCIATED CONTENT

S Supporting Information. Figures showing the M05-2X and B3LYP optimized geometries of the stationary points coming from the reaction between the anion of caffeic acid and the hydroxyl radical, for HAT, RAF, and SET mechanisms. Tables reporting the atomic spin densities at the M05-2X level

in the products coming from HAT, RAF, and SET mechanisms. Figures showing the minimum energy path and the adiabatic potential-energy profiles computed at the M052X level for the HAT and RAF mechanisms. Complete refs 97 and 98. This material is available free of charge via the Internet at <http://pubs.acs.org>.

AUTHOR INFORMATION

Corresponding Author

*E-mail: nrusso@unical.it.

ACKNOWLEDGMENT

The University of Calabria and the Food Science & Engineering Interdepartmental Center of the University of Calabria, L.I.P.A.C., Calabrian Laboratory of Food Process Engineering (Regione Calabria APQ—Ricerca Scientifica e Innovazione Tecnologica I atto integrativo, Azione 2 laboratori pubblici di ricerca mission oriented interfiliere), and FONCICYT Mexico—EU "RMAYS" network, Project No. 94666, are gratefully acknowledged.

REFERENCES

- (1) Hertog, M. G. L.; Hollman, P. C. H.; Katan, M. B.; Kromhout, D. Intake of potentially anticarcinogenic flavonoids and their determinants in adults in the Netherlands. *Nutr. Cancer* **1993**, *20*, 21.
- (2) Robak, J.; Gryglewski, R. J. Bioactivity of flavonoids. *Pol. J. Pharmacol.* **1996**, *48*, 555.
- (3) Clifford, M. N. Chlorogenic acids and other cinnamates — nature, occurrence and dietary burden. *J. Sci. Food Agric.* **1999**, *79*, 362.
- (4) Rice-Evans, C.; Spencer, J. E.; Schroeter, H.; Rechner, A. R. Bioavailability of Flavonoids and Potential Bioactive Forms in Vivo. *Drug Metab. Drug Interact.* **2000**, *17*, 291.
- (5) Rencher, A. R.; Spencer, P. E.; Kuhnle, G.; Hahn, U.; Rice-Evans, C. A. Novel biomarkers of the metabolism of caffeic acid derivatives in vivo. *Free Radical Biol. Med.* **2001**, *30*, 1213.
- (6) Brit, D. F.; Hendrich, S.; Wang, W. Dietary agents in cancer prevention: flavonoids and isoflavonoids. *Pharmacol. Ther.* **2001**, *90*, 157.
- (7) Ross, J. A.; Kasum, C. M. DIETARY FLAVONOIDS: Bioavailability, Metabolic Effects, and Safety. *Ann. Rev. Nutr.* **2002**, *22*, 19.
- (8) Kris-Etherton, P. M.; Hecker, K. D.; Bonanome, A. B.; Coval, S. M.; Binkoski, A. E.; Hilpert, K.; Griel, A. E.; Etherton, T. D. Bioactive compounds in foods: their role in the prevention of cardiovascular disease and cancer. *Am. J. Med.* **2002**, *113*, 71.
- (9) Bravo, L. Polyphenols: Chemistry, Dietary Sources, Metabolism, and Nutritional Significance. *Nutr. Rev.* **1998**, *56*, 317.
- (10) Harborne, J. B. In *Plant Flavonoids in Biology and Medicine 11: Biochemical, Cellular and Medicinal Properties*; Alan R. Liss: New York, 1988; p 17.
- (11) Swain, T. In *Plant Flavonoids in Biology and Medicine: Biochemical, Pharmacological, and Structure-Activity Relationships*; Alan R. Liss: New York, 1986; p 1.
- (12) Harborne, J. B. In *Plant Flavonoids in Biology and Medicine: Biochemical Pharmacological, and Structure-Activity Relationships*; Alan R. Liss: New York, 1986; p 15.
- (13) Renaud, S.; de Lorgeril, M. Wine, alcohol, platelets, and the French paradox for coronary heart disease. *Lancet* **1992**, *339*, 1523.
- (14) Frankel, E. N.; Kanner, J.; German, J. B.; Parks, E.; Kinsella, J. E. Inhibition of oxidation of human low-density lipoprotein by phenolic substances in red wine. *Lancet* **1993**, *341*, 454.
- (15) Robbins, R. J. Phenolic acids in foods: an overview of analytical methodology. *J. Agric. Food Chem.* **2003**, *51*, 2866.
- (16) King, A.; Young, G. Characteristics and Occurrence of Phenolic Phytochemicals. *J. Am. Diet. Ass.* **1999**, *99*, 213.
- (17) Cody, V.; Middleton, E.; Harborne, J. B. In *Plant Flavonoids in Biology and Medicine-Biochemical, Pharmacological and structure-activity relationships*; Alan R. Liss: New York, 1986; p 429.
- (18) Cody, V.; Middleton, E.; Harborne, J. B.; Beretz, A. In *Plant Flavonoids in Biology and Medicine II-Biochemical, Cellular and Medicinal Properties*; Alan R. Liss: New York, 1988; p 187.
- (19) Das, N. P. In *Flavonoids in Biology and Medicine III-Current Issues in Flavonoids Research*; Singapore University Press: Singapore, 1990; p 213.
- (20) Kandaswami, C.; Middleton, E. Free radical scavenging and antioxidant activity of plant flavonoids. *Adv. Exp. Med. Biol.* **1994**, *366*, 351.
- (21) Duarte, J.; Perez-Vizcaínom, F.; Utrilla, P.; Jiminez, J.; Tanargo, J.; Zarzuelo, A. Vasodilatory effects of flavonoids in rat aortic smooth muscle. Structure-activity relationships. *Gen. Pharmacol.* **1993**, *24*, 857.
- (22) Duarte, J.; Perez-Vizcaínom, F.; Zarzuelo, A.; Jiminez, J.; Tanargo, J. Vasodilator effects of quercetin in isolated rat vascular smooth muscle. *Eur. J. Pharmacol.* **1993**, *239*, 1.
- (23) Brown, J. P. A review of the genetic effects of naturally occurring flavonoids, anthraquinones and related compounds. *Mut. Res.* **1980**, *75*, 243.
- (24) Mabry, T. J.; Markham, K. R.; Chari, V. M. In *The Flavonoids. Advances in Research*; Harborne, J. R., Mabry, T. J., Eds.; Chapman and Hall: London, 1982; p 52.
- (25) Robak, J.; Shridi, F.; Wolbis, M.; Krolikowska, M. Screening of the influence of flavonoids on lipoxygenase and cyclooxygenase activity. *Pol. J. Pharmacol. Pharm.* **1988**, *40*, 451.
- (26) Ho, C.-T.; Chen, Q.; Shi, H.; Zhang, K.-Q.; Rosen, R. T. Antioxidative effect of polyphenol extract prepared from various Chinese teas. *Prev. Med.* **1992**, *21*, 520.
- (27) Middleton, E.; Kandaswami, C. Effects of flavonoids on immune and inflammatory cell functions. *Biochem. Pharmacol.* **1992**, *43*, 1167.
- (28) Jovanovic, S. V.; Jankovic, I.; Josimovic, L. Electron-Transfer Reactions of Alkyl Peroxy Radicals. *J. Am. Chem. Soc.* **1992**, *114*, 9018.
- (29) Sogawa, S.; Nihro, Y.; Ueda, H.; Uzumi, A.; Miki, T.; Matsumoto, H.; Satoh, T. 3,4-Dihydroxychalcones as Potent 5-Lipoxygenase and Cyclooxygenase Inhibitors. *J. Med. Chem.* **1993**, *36*, 3904.
- (30) Lindahl, M.; Tagesson, C. Selective inhibition of group II phospholipase A₂ by quercetin. *Inflammation* **1993**, *17*, 573.
- (31) Elliot, A. J.; Scheiber, S. A.; Thomas, C.; Pardini, R. S. Inhibition of glutathione reductase by flavonoids: A structure-activity study. *Biochem. Pharmacol.* **1992**, *44*, 1603.
- (32) Chang, W. S.; Lee, Y. J.; Lu, F. J.; Chang, H. C. Inhibitory effects of flavonoids on xanthine oxidase. *Anticancer Res.* **1993**, *13*, 2165.
- (33) Report of the joint WHO/FAO expert consultation. Diet, nutrition and the prevention of chronic diseases. WHO Technical Report Series, No. 916 (TRS916), 2003.
- (34) de Groot, H. Reactive oxygen species in tissue injury. *Hepato-gastroenterol.* **1994**, *41*, 328.
- (35) Grace, P. A. Ischaemia-reperfusion injury. *Brit. J. Surg.* **1994**, *81*, 637.
- (36) Halliwell, B. How to characterize an antioxidant: an update. *Biochem. Soc. Symp.* **1995**, *61*, 73.
- (37) Darias-Martin, J.; Martin-Luis, B.; Carrillo-Lopez, M.; Lamuela-Raventos, R.; Diaz-Romero, C.; Boulton, R. Effect of Caffeic Acid on the Color of Red Wine. *J. Agric. Food Chem.* **2002**, *50*, 2062.
- (38) Gulcin, I. Antioxidant activity of caffeic acid (3,4-dihydroxycinnamic acid). *Toxicology* **2006**, *217*, 213.
- (39) Kroon, P. A.; Williamson, G. Hydroxycinnamates in plants and food: current and future perspectives. *J. Sci. Food Agric.* **1999**, *79*, 355.
- (40) Fukumoto, L. R.; Mazza, G. Assessing Antioxidant and Prooxidant Activities of Phenolic Compounds. *J. Agric. Food Chem.* **2000**, *48*, 3597.
- (41) Frank, H.; Thiel, D.; Macleod, J. Mass spectrometric detection of cross-linked fatty acids formed during radical-induced lesion of lipid membranes. *Biochem. J.* **1989**, *260*, 873.
- (42) Gebhardt, R.; Fausel, M. Antioxidant and hepatoprotective effects of artichoke extract and constituents in cultured rat hepatocytes. *Toxicology* **1997**, *11*, 669.
- (43) Joyeux, M.; Lobstein, A.; Anton, R.; Mortier, F. Comparative antilipoperoxidant, antinecrotic and scavenging properties of terpenes and biflavones from Ginkgo and some flavonoids. *Planta Med.* **1995**, *61*, 126.

- (44) Challis, B. C.; Bartlett, C. D. Possible cocarcinogenic effects of coffee constituents. *Nature* **1975**, *254*, 532.
- (45) Iwahashi, H.; Ishii, T.; Sugata, R.; Kido, R. The effects of caffeic acid and its related catechols on hydroxyl radical formation by 3-hydroxyanthranilic acid, ferric chloride, and hydrogen peroxide. *Arch. Biochem. Biophys.* **1990**, *276*, 242.
- (46) Sudina, G. F.; Mirzoeva, O. K.; Pushkareva, M. A.; Korshunova, G. A.; Sumbatyan, N. V.; Varfolomeev, S. D. Caffeic acid phenethyl ester as a lipoxygenase inhibitor with antioxidant properties. *FEBS Lett.* **1993**, *329*, 21.
- (47) Rao, M. V.; Paliyath, G.; Ormrod, D. P. Ultraviolet-B- and Ozone-Induced Biochemical Changes in Antioxidant Enzymes of *Arabidopsis thaliana*. *Plant Physiol.* **1996**, *110*, 125.
- (48) Meyer, A. S.; Donovan, J. L.; Pearson, D. A.; Waterhouse, A. L.; Frankel, E. N. Fruit Hydroxycinnamic Acids Inhibit Human Low-Density Lipoprotein Oxidation in Vitro. *J. Agric. Food Chem.* **1998**, *46*, 1783.
- (49) Cartron, E.; Carboneau, M. A.; Fouret, G.; Descomps, B.; Leger, C. L. Specific Antioxidant Activity of Caffeoyl Derivatives and Other Natural Phenolic Compounds: LDL Protection against Oxidation and Decrease in the Proinflammatory Lysophosphatidylcholine Production. *J. Nat. Prod.* **2001**, *64*, 480.
- (50) Kikuzaki, H.; Hisamoto, M.; Hirose, K.; Akiyama, K.; Taniguchi, H. Antioxidant Properties of Ferulic Acid and Its Related Compounds. *J. Agric. Food Chem.* **2002**, *50*, 2161.
- (51) Wright, J. S.; Johnson, E. R.; Di Labio, G. A. Predicting the Activity of Phenolic Antioxidants: Theoretical Method, Analysis of Substituent Effects, and Application to Major Families of Antioxidants. *J. Am. Chem. Soc.* **2001**, *123*, 1173.
- (52) Leopoldini, M.; Prieto Pitarch, I.; Russo, N.; Toscano, M. Structure, Conformation, and Electronic Properties of Apigenin, Luteolin, and Taxifolin Antioxidants. A First Principle Theoretical Study. *J. Phys. Chem. A* **2004**, *108*, 92.
- (53) Leopoldini, M.; Marino, T.; Russo, N.; Toscano, M. Density functional computations of the energetic and spectroscopic parameters of quercetin and its radicals in the gas phase and in solvent. *Theor. Chem. Acc.* **2004**, *111*, 210.
- (54) Leopoldini, M.; Marino, T.; Russo, N.; Toscano, M. Antioxidant Properties of Phenolic Compounds: H-Atom versus Electron Transfer Mechanism. *J. Phys. Chem. A* **2004**, *108*, 4916.
- (55) Jovanovic, S. V.; Steenken, S.; Simic, M. G.; Hara, Y. In *Flavonoids in Health and Disease*; Rice-Evans, C., Packer, L., Eds.; Marcel Dekker: New York, 1998; p 137.
- (56) Leopoldini, M.; Russo, N.; Chiodo, S.; Toscano, M. Iron Chelation by the Powerful Antioxidant Flavonoid Quercetin. *J. Agric. Food Chem.* **2006**, *54*, 6343.
- (57) Belyakov, V. A.; Roginsky, V. A.; Bors, W. Rate constants for the reaction of peroxy radical with flavonoids and related compounds as determined by the kinetic chemiluminescence method. *J. Chem. Soc., Perkin Trans. 2* **1995**, 2319.
- (58) Kono, Y.; Kobayashi, K.; Tagawa, S.; Adachi, K.; Ueda, A.; Sawa, Y.; Shibata, H. Antioxidant activity of polyphenolics in diets: Rate constants of reactions of chlorogenic acid and caffeic acid with reactive species of oxygen and nitrogen. *Biochim. Biophys. Acta* **1997**, *1335*, 335.
- (59) Foley, S.; Navaratnam, S.; McGarvey, D. J.; Land, E. J.; Truscott, T. G.; Rice-Evans, C. A. Singlet oxygen quenching and the redox properties of hydroxycinnamic acids. *Free Radical Biol. Med.* **1999**, *26*, 1202.
- (60) Lu, Y.; Foo, L. Y. Salvianolic acid L, a potent phenolic antioxidant from *Salvia officinalis*. *Tetrahedron Lett.* **2001**, *42*, 8223.
- (61) Lu, Y.; Foo, L. Y. Antioxidant activities of polyphenols from sage (*Salvia officinalis*). *Food Chem.* **2001**, *75*, 197.
- (62) Becke, A. D. Density-functional thermochemistry. III. The role of exact exchange. *J. Chem. Phys.* **1993**, *98*, 5648.
- (63) Lee, C.; Yang, W.; Parr, R. G. Development of the Colle-Salvetti correlation-energy formula into a functional of the electron density. *Phys. Rev. B* **1988**, *37*, 785.
- (64) Becke, A. D. A new mixing of Hartree-Fock and local density-functional theories. *J. Chem. Phys.* **1993**, *98*, 1372.
- (65) Becke, A. D. Density-functional exchange-energy approximation with correct asymptotic behavior. *Phys. Rev. A* **1988**, *38*, 3098.
- (66) Zhao, Y.; Schultz, N. E.; Truhlar, D. G. Design of Density Functionals by Combining the Method of Constraint Satisfaction with Parametrization for Thermochemistry, Thermochemical Kinetics, and Noncovalent Interactions. *J. Chem. Theory Comput.* **2006**, *2*, 364.
- (67) Ditchfield, R.; Hehre, W. J.; Pople, J. A. Self-Consistent Molecular-Orbital Methods. IX. An Extended Gaussian-Type Basis for Molecular-Orbital Studies of Organic Molecules. *J. Chem. Phys.* **1971**, *54*, 724.
- (68) Hehre, W. J.; Ditchfield, R.; Pople, J. A. Self-Consistent Molecular Orbital Methods. XII. Further Extensions of Gaussian-Type Basis Sets for Use in Molecular Orbital Studies of Organic Molecules. *J. Chem. Phys.* **1972**, *56*, 2257.
- (69) Hariharan, P. C.; Pople, J. A. Accuracy of AH equilibrium geometries by single determinant molecular-orbital theory. *Mol. Phys.* **1974**, *27*, 209.
- (70) Gordon, M. S. The isomers of silacyclopropane. *Chem. Phys. Lett.* **1980**, *76*, 163.
- (71) Zavala-Oseguera, C.; Alvarez-Idaboy, J. R.; Merino, G.; Galano, A. OH Radical Gas Phase Reactions with Aliphatic Ethers: A Variational Transition State Theory Study. *J. Phys. Chem. A* **2009**, *113*, 13913.
- (72) Velez, E.; Quijano, J.; Notario, R.; Pabon, E.; Murillo, J.; Leal, J.; Zapata, E.; Alarcon, G. A computational study of stereospecificity in the thermal elimination reaction of menthyl benzoate in the gas phase. *J. Phys. Org. Chem.* **2009**, *22*, 971.
- (73) Vega-Rodriguez, A.; Alvarez-Idaboy, J. R. Quantum chemistry and TST study of the mechanisms and branching ratios for the reactions of OH with unsaturated aldehydes. *Phys. Chem. Chem. Phys.* **2009**, *11*, 7649.
- (74) Galano, A.; Alvarez-Idaboy, J. R. Guanosine + OH radical reaction in aqueous solution: A reinterpretation of the UV-Vis data based on thermodynamic and kinetic calculations. *Org. Lett.* **2009**, *11*, 5114.
- (75) Black, G.; Simmie, J. M. Barrier heights for H-atom abstraction by HO₂[·] from n-butanol—a simple yet exacting test for model chemistries? *J. Comput. Chem.* **2010**, *31*, 1236.
- (76) Furuncuoglu, T.; Ugur, I.; Degirmenci, I.; Aviyente, V. Role of Chain Transfer Agents in Free Radical Polymerization Kinetics. *Macromolecules* **2010**, *43*, 1823.
- (77) Galano, A.; Macías-Ruvalcaba, N. A.; Campos, O. N. M.; Pedraza-Chaverri, J. Mechanism of the OH Radical Scavenging Activity of Nordihydroguaiaretic Acid: A Combined Theoretical and Experimental Study. *J. Phys. Chem. B* **2010**, *114*, 6625.
- (78) Truhlar, D. G.; Kupperman, A. Exact tunneling calculations. *J. Am. Chem. Soc.* **1971**, *93*, 1840.
- (79) Fukui, K. Chemical reactivity theory - its pragmatism and beyond. *Pure Appl. Chem.* **1982**, *54*, 1825.
- (80) Miertus, S.; Scrocco, E.; Tomasi, J. Electrostatic interactions of a solute with a continuum. A direct utilization of ab initio molecular potentials for the prevision of solvent effects. *Chem. Phys.* **1981**, *55*, 117.
- (81) Miertus, S.; Tomasi, J. Approximate Evaluations of the Electrostatic Free Energy and Internal Energy Changes in Solution Processes. *Chem. Phys.* **1982**, *65*, 239.
- (82) Cossi, M.; Barone, V.; Cammi, R.; Tomasi, J. Ab initio study of solvated molecules: a new implementation of the polarizable continuum model. *Chem. Phys. Lett.* **1996**, *255*, 327.
- (83) Barone, V.; Cossi, M.; Menucci, B.; Tomasi, J. A new definition of cavities for the computation of solvation free energies by the polarizable continuum model. *J. Chem. Phys.* **1997**, *107*, 3210.
- (84) Garrett, B. C.; Truhlar, D. G. Criterion of minimum state density in the transition state theory of bimolecular reactions. *J. Chem. Phys.* **1979**, *70*, 1593.
- (85) Garrett, B. C.; Truhlar, D. G.; Grev, R. S.; Magnuson, A. W. Improved Treatment of Threshold Contributions in Variational Transition State Theory. *J. Phys. Chem.* **1980**, *84*, 1730.
- (86) Isaacson, A. D.; Truhlar, D. G. Polyatomic Canonical Variational Theory for Chemical Reaction Rates. Separable-Mode Formalism with Application to OH + H₂ → H₂O + H. *J. Chem. Phys.* **1982**, *76*, 1380.

- (87) Truhlar, D. G.; Isaacson, A. D.; Garrett, B. C. In *Theory of Chemical Reaction Dynamics*; Baer, M., Ed.; CRC Press: Boca Raton, FL, 1985; Vol. 4, p 65.
- (88) Fernandez-Ramos, A.; Miller, J. A.; Klippenstein, S. J.; Truhlar, D. G. Modeling of Bimolecular Reactions. *Chem. Rev.* **2006**, *106*, 4518.
- (89) Liu, Y. P.; Lynch, G. C.; Truong, T. N.; Lu, D. H.; Truhlar, D. G.; Garrett, P. C. Molecular Modeling of the Kinetic Isotope Effect for the [1,5]-Sigmatropic Rearrangement of *cis*-1,3-Pentadiene. *J. Am. Chem. Soc.* **1993**, *115*, 2408.
- (90) Lu, D. H.; Truong, T. N.; Melissas, V.; Lynch, G. C.; Liu, Y. P.; Garrett, B. C.; Steckler, R.; Isaacson, A. D.; Rai, S. N.; Hancock, G. C.; Laurerdale, J. G.; Joseph, T.; Truhlar, D. G. POLYRATE 4: A New Version of a Computer Program for the Calculation of Chemical Reaction Rates for Polyatomics. *Comput. Phys. Commun.* **1992**, *71*, 235.
- (91) Truhlar, D. G.; Gordon, M. S. From Force Fields to Dynamics: Classical and Quantal Paths. *Science* **1990**, *249*, 491.
- (92) Truong, T. N.; Lu, D. H.; Lynch, G. C.; Liu, Y. P.; Melissas, V.; Stewart, J. P.; Steckler, R.; Garrett, B. C.; Isaacson, A. D.; Gonzalez-Lafont, A.; Rai, S. N.; Hancock, G. C.; Joseph, T.; Truhlar, D. G. MORATE: A Program for Direct Dynamics Calculations of Chemical Reaction Rates by Semiempirical Molecular Orbital Theory. *Comput. Phys. Commun.* **1993**, *75*, 143.
- (93) Espinosa-Garcia, J. Theoretical Study of the Trapping of the OOH Radical by Coenzyme Q. *J. Am. Chem. Soc.* **2004**, *126*, 920.
- (94) Navarrete, M.; Rangel, C.; Espinosa-Garcia, J.; Corchado, J. C. Theoretical Study of the Antioxidant Activity of Vitamin E: Reactions of α -Tocopherol with the Hydroperoxy Radical. *J. Chem. Theory Comput.* **2005**, *1*, 337.
- (95) Tejero, I.; Gonzalez-Garcia, N.; Gonzalez-Lafont, A.; Lluch, J. M. Tunneling in Green Tea: Understanding the Antioxidant Activity of Catechol-Containing Compounds. A Variational Transition-State Theory Study. *J. Am. Chem. Soc.* **2007**, *129*, 5846.
- (96) Chioldo, S. G.; Leopoldini, M.; Russo, N.; Toscano, M. The inactivation of lipid peroxide radical by quercetin. A theoretical insight. *Phys. Chem. Chem. Phys.* **2010**, *12*, 7662.
- (97) Frisch, M. J.; et al. *Gaussian 03*; Gaussian, Inc.: Pittsburgh PA, 2003.
- (98) Corchado, J. C.; et al. POLYRATE, version 9.7; University of Minnesota, Minneapolis, MN, 2007.
- (99) Zhao, Y.; Truhlar, D. G. Benchmark Databases for Nonbonded Interactions and Their Use To Test Density Functional Theory. *J. Chem. Theory Comput.* **2005**, *1*, 415.
- (100) Leopoldini, M.; Russo, N.; Toscano, M. The molecular basis of working mechanism of natural polyphenolic antioxidants. *Food Chem.* **2011**, *125*, 288.
- (101) Sousa, S. F.; Fernandes, P. A.; Ramos, M. J. General Performance of Density Functionals. *J. Phys. Chem. A* **2007**, *111*, 10439 and references therein.
- (102) Zhao, Y.; Gonzalez-Garcia, N.; Truhlar, D. G. Benchmark Database of Barrier Heights for Heavy Atom Transfer, Nucleophilic Substitution, Association, and Unimolecular Reactions and Its Use to Test Theoretical Methods. *J. Phys. Chem. A* **2005**, *109*, 2012.
- (103) Bors, W.; Michel, C.; Stettmaier, K.; Lu, Y.; Foo, L. Y. Pulse radiolysis, electron paramagnetic resonance spectroscopy and theoretical calculations of caffeic acid oligomer radicals. *Biochim. Biophys. Acta* **2003**, *1620*, 97.
- (104) Li, X. F.; Cai, Z. L.; Katsumura, Y.; Wu, G. Z.; Muroya, Y. Reactions of reducing and oxidizing radicals with caffeic acid: a pulse radiolysis and theoretical study. *Radiat. Phys. Chem.* **2001**, *60*, 345.
- (105) Wang, W. F.; Luo, J.; Yao, S. D.; Lian, Z. R.; Zhang, J. S.; Lin, N. Y.; Fang, R. Y.; Hu, T. X. Interaction of phenolic antioxidants and hydroxyl radicals. *Radiat. Phys. Chem.* **1993**, *42*, 985.